Epileptic seizure prediction from eigen-wavelet multivariate self-similarity analysis of multi-channel EEG signals

Charles-Gérard Lucas, Patrice Abry
ENSL, CNRS, Laboratoire de physique, F-69342 Lyon, France.
firstname.lastname@ens-lyon.fr

Herwig Wendt
IRIT, Univ. Toulouse, CNRS, Toulouse, France.
herwig.wendt@irit.fr

Gustavo Didier
Math. Dept.,Tulane University, New Orleans, USA
gdidier@tulane.edu

***Abstract*—Epileptic patients can undergo severe brain damages during seizures. There is thus a significant need for automated seizure prediction. Brain activity has been shown to display a scale-free temporal dynamics, which has, in turn, been involved in seizure prediction. Self-similarity, the paradigm model for scale-free dynamics, has however mostly been studied in univariate settings, considering recorded signals independently. Yet, non-negligible correlations exist in multi-channel recordings of brain activity and must be accounted for. The present work aims to assess the relevance and benefits of a recently developed multivariate eigen-wavelet framework for multivariate self-similarity analysis in seizure prediction using CHB-MIT Scalp EEG data.**

***Index Terms*—Multivariate self-similarity, multivariate wavelet transform, EEG data, Epilepsy, seizure prediction.**

I. Introduction

Context. Epilepsy, a chronic disease consists of a central nervous system disorder, leading to seizures during which the patient brain can be severely injured. Devising automated epileptic seizure prediction procedures thus constitutes a crucial and on-going stake, notably when they can be implemented from non-invasive and wearable scalp EEG devices.

It was shown in many studies that brain activity can be well-described by arrhythmic or scale-free dynamics efficiently modeled by self-similarity [1], [2]. In practice, self-similarity analysis relies on the estimation of the self-similarity or Hurst exponent [3], [4]. Self-similarity is mostly studied in univariate settings, i.e., self-similarity exponents are estimated independently for each time series. However, brain activity is monitored via numerous sensors, yielding multivariate time series recorded jointly. Recently, a multivariate self-similarity model, operator fractional Brownian motion (ofBm) was proposed and a corresponding multivariate eigen-wavelet-based analysis was developed [4]. The present work aims to quantify the relevance and benefits of multivariate self-similarity analysis in brain activity monitoring through the prediction of epileptic seizures from scalp EEG data.

Related works. Seizure prediction constitutes an important research topic, often investigated using tools such as synchronization and functional connectivity [5], phase coherence [6], power spectral density [7] or power of the wavelet coefficients [8] in standard frequency bands, autoregressive models [9], or more recently deep learning frameworks [10]. Scale-free dynamics have also been involved in seizure prediction (e.g., from intracranial EEG [11] or single scalp EEG [12]). Fractional Brownian motion (fBm) has been shown to be a relevant model for scale-free temporal dynamics [3] and often used to analyze MEG and EEG data analysis. Most works however rely on univariate self-similarity (or multifractal) analysis. In the context of scalp EEG data, multivariate self-similarity models such as ofBm [4], [13] could prove more efficient to account for cross-temporal dynamics in EEG time series. This has so far never been tried.

Goals, contributions and outline. The present work aims to quantify the relevance and benefits of using multivariate self-similarity models and eigen-wavelet-based analysis in epilepsy seizure prediction from multi-channel scalp EEG data. Section II describes the ofBm model and multivariate wavelet spectrum eigenvalues-based analysis for M-variate fBm through the estimation of M self-similarity exponents. This tool is applied to $M = 22$-variate EEG data, obtained from the CHB-MIT Scalp EEG database, documented in [14] as described in Section III. Finally, Section IV quantifies the significance of multivariate self-similarity analysis for epileptic seizure prediction.

II. Multivariate self-similarity

Operator fractional Brownian motion. Fractional Brownian motion (fBm), the only Gaussian, self-similar stochastic process with stationary increments, is a classical model for univariate self-similarity [3], [4]. To analyze the multivariate times series conveying brain activity, it can be modeled as a collection of possibly correlated M-fBm $X \triangleq \{X_{H_1}(t), \ldots, X_{H_M}(t)\}_{t\in\mathbb{R}}$ each associated with a possibly different self-similarity parameter H_m. Further, these M-fBm are possibly linearly mixed via a $M \times M$ real-valued invertible matrix W, $Y \triangleq WX = W\ \{X_{H_1}(t), \ldots, X_{H_M}(t)\}_{t\in\mathbb{R}}$. The resulting multivariate process Y is a specific case of *operator fractional*

Supported by PhD Grant DGA/AID (no 01D20019023), ANR-16-CE33-0020 MultiFracs, ANR-18-CE45-0007 MUTATION. G. Didier's long term visits to ENS Lyon were sponsored by ENS Lyon, the CNRS and the Simons Foundation collaboration grant #714014.

Brownian motion [4]. Multivariate self-similarity analysis thus amounts to estimating, from the observation of Y, the vector of self-similarity parameters $\underline{H} = (H_1, \ldots, H_M)$.

Multivariate wavelet analysis. In the present work, self-similarity is analyzed through a wavelet-based representation. Let $D_{Y_m}(2^j, k) = \langle 2^{-j/2}\psi_0(2^{-j}t - k)|Y_m(t)\rangle$, $\forall k \in \mathbb{Z}$, $\forall j \in \{j_1, \ldots, j_2\}$ denote the discrete wavelet transform (DWT) coefficients of component Y_m, where ψ_0 stands for the reference mother wavelet [15]. Multivariate DWT is defined naturally as the collection of univariate DWT of each component Y_m, using the same mother wavelet. This amounts to concatenate the univariate DWT coefficients into $D_Y(2^j, k) = (D_{Y_1}(2^j, k), \ldots, D_{Y_M}(2^j, k))$, $\forall k \in \mathbb{Z}$, $\forall j \in \{j_1, \ldots, j_2\}$, $\forall m \in \{1, \ldots, M\}$. The wavelet spectrum is then defined as the collection of covariance matrices of $D_Y(2^j, k)$, computed independently at scale 2^j:

$$S(2^j) \triangleq \frac{1}{n_j} \sum_{k=1}^{n_j} D_Y(2^j, k) D_Y(2^j, k)^*. \quad (1)$$

Self-similarity analysis consists in the estimation of the exponents $\underline{H} = (H_1, \ldots, H_M)$ from the M-variate time series Y.

Univariate self-similarity analysis. First, M independent univariate analyses can be conducted from using only the diagonal entries $S_{m,m}(2^j)$ of the wavelet spectrum. When there is no mixing, ($W \equiv I$), the $S_{m,m}(2^j)$ asymptotically behave as power-laws, with scaling exponent $2H_m - 1$, thus leading to a linear regression based estimator of H_m [4]:

$$\hat{H}_m^U = \left(\sum_{j=j_1}^{j_2} v_j S_{m,m}(2^j) \right) / 2 - \frac{1}{2}, \quad m = 1, \ldots, M, \quad (2)$$

with v_j classical regression weights such that $\sum_j j v_j = 1$ and $\sum_j v_j = 0$ (cf. [4]). Obviously, these M-univariate analyses lead to biased estimation of the self-similarity parameters when linear mixing is present ($W \neq I$), and even without mixing do not exploit cross temporal dynamics likely to exist in data.

Classical multivariate self-similarity analysis. To account for cross-temporal dependencies amongst components, the non diagonal entries $S_{m,m'}(2^j)$ ($m' \neq m$) of the wavelet spectrum can be used. Without mixing, the $S_{m,m'}(2^j)$ asymptotically behave as power-laws, with scaling exponent $2H_{m,m'} - 1$, with $H_{m,m'} = (H_m + H_{m'})/2$. This naturally leads to estimate $H_{m,m'}$ by a linear regression:

$$\hat{H}_{m,m'} = \left(\sum_{j=j_1}^{j_2} v_j S_{m,m'}(2^j) \right) / 2 - \frac{1}{2}, \quad m \leq m' = 1, \ldots, M. \quad (3)$$

Obviously, these $M(M-1)/2$ estimates lead to biased estimation of $\underline{H}$ when linear mixing is present ($W \neq I$). Further, without mixing, departures of $\hat{H}_{m,m'}$ from $(H_m + H_{m'})/2$ may quantify departures of data from the underlying ofbm model, a potentially valuable multivariate information.

Eigen-wavelet multivariate self-similarity analysis. To account both for cross-dependencies and mixing, an alternative *eigen-wavelet* based multivariate selsimilarity analysis was proposed [4]. It shows that each of the eigenvalues $\lambda_m(2^j)$ of the wavelet spectrum $S(2^j)$ asymptotically behaves as power law with respect to the scales 2^j, with scaling exponent $2H_m - 1$, with and without mixing.

This naturally suggests to perform the practical estimation of H_m by a linear regression of $\log_2 \lambda_m(2^j)$ against octaves $j = \log_2 2^j$. However, this would results in significant biases because of the so-called *repulsion effect* altering the estimation of covariance matrix eigen-values from finite size observations. By nature of multiscale analysis, that bias increases at coarser scales [13]. To overcome this bias, it was proposed to compute several wavelet spectra, from non overlapping time windows $w = 1, \ldots, 2^{j-j_2}$, using an identical number of wavelet coefficients common to all scales 2^j [13]:

$$S^{(w)}(2^j) \triangleq \frac{1}{n_{j_2}} \sum_{k=1+(w-1)n_{j_2}}^{wn_{j_2}} D_Y(2^j, k) D_Y(2^j, k)^*. \quad (4)$$

The eigenvalues $\{\lambda_1^{(w)}(2^j), \ldots, \lambda_M^{(w)}(2^j)\}$ of $S^{(w)}(2^j)$ are computed for each non-overlapping window w at each scale 2^j, entailing a repulsion effect of similar size at all scales, thus leading to an unbiased estimation of H_m. In practice, the $H_1, \ldots, H_M$ are thus estimated by means of linear regressions over the octaves j of the log-averaged eigenvalues $\log_2 \bar{\lambda}_m(2^j) \triangleq 2^{j_2 - j} \sum_{w=1}^{2^{j-j_2}} \log_2(\lambda_m^{(w)}(2^j))$:

$$\hat{H}_m^M = \left(\sum_{j=j_1}^{j_2} v_j \log_2 \bar{\lambda}_m(2^j) \right) / 2 - \frac{1}{2}, \quad m = 1, \ldots, M. \quad (5)$$

This estimation procedure was assessed on synthetic M-fBm in [13].

III. Epilepsy dataset

Data description. Data used in this work consist of multichannel scalp EEG recordings from the CHB-MIT Scalp EEG database available at https://physionet.org/content/chbmit/1.0.0/, documented in [14]. These recordings have been collected at the Boston Children's Hospital from pediatric subjects with intractable seizures and sampled at 256Hz.

EEG recordings have been divided into 23 cases collected from 22 subjects, composed of 5 males and 17 females, annotated with beginnings and ends of epileptic seizures. For each case, between 22 and 26 EEG signals have been recorded for several hours according to the International 10-20 system of EEG electrode positions and nomenclature. The recordings are at least one-hour long and only a part of them contains seizures.

Data preprocessing. In the present work, we make use of the 22 first EEG channels, so as to use the same channels for all subjects.

Because the work focuses on predicting epilepsy, the goal is to perform a detection of preictal states, which are periods occurring a few minutes before the onset of an epileptic seizure. Thus windows corresponding to preictal states are selected in the recordings containing seizures while windows

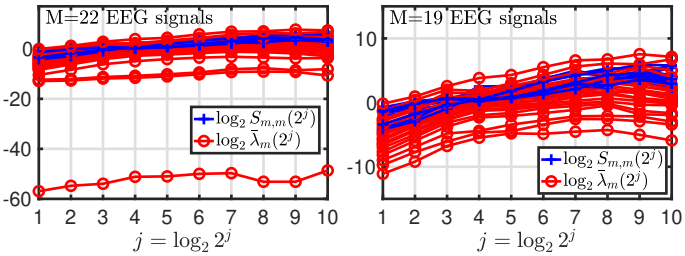

Fig. 1. **Multivariate scale-free analysis.** Diagonal entries $\log_2 S_{m,m}(2^j)$ (blue '+') and log-eigenvalues $\log_2 \bar{\lambda}_m(2^j)$ (red 'o') of the wavelet spectrum $S(2^j)$ for one preictal window associated with Subject 5 before (left) and after (right) removal of 3 redundant channels.

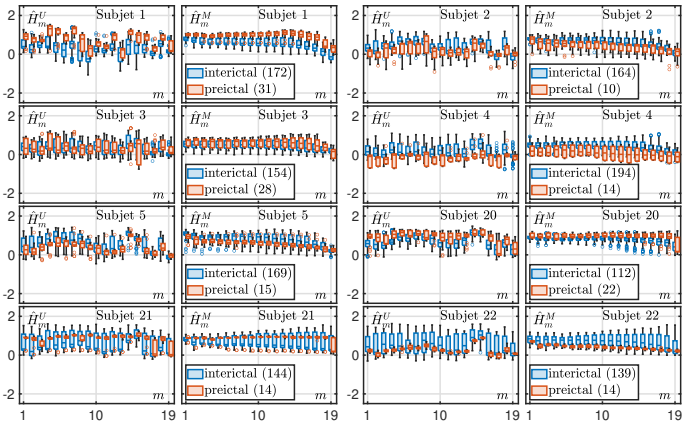

Fig. 2. **Distributions of estimated self-similarity parameters.** Boxplots for the univariate estimates $\hat{H}_m^U$ (left) and multivariate estimates $\hat{H}_m^M$ (right) for preictal (red) and interictal (blue) states, for all subjects.

corresponding to interictal states (far in time from any epilectic seizure) are selected in the recordings with no seizure. In practice, 2-minute long windows ($30,720$ samples) are used.

To assess quantitatively the performance of the proposed multivariate eigen-wavelet based self-similarity analysis to detect preictal states, only subjects with at least 110 interictal and 10 preictal windows are considered. Thus, only 8 subjects are studied in this work.

IV. Prediction of Preictal States

A. Analysis set-up

The 2-minute long windows of the EEG signals are analysed using Daubechies wavelets with $N_\psi = 2$ vanishing moments. Linear regressions are performed across scales 2^1 to 2^4, corresponding to equivalent frequencies ranging from 10Hz to 85Hz, where intracranial EEG signals are documented to have scale-free dynamics [11].

B. Single window multivariate analysis

Fig. 1(left) compares, for a preictal window of a given subject, the $M = 22$-univariate wavelet analysis $\log_2 S_{m,m}(2^j)$ (solid black lignes with '+') against the eigen-wavelet based multivariate analysis $\log_2 \bar{\lambda}_m(2^j)$ (solid red lines with 'o'). While the $M = 22$-univariate $\log_2 S_{m,m}(2^j)$ functions mostly superimpose, the multivariate eigen-value based analysis clearly shows that three eigen functions $\log_2 \bar{\lambda}_m(2^j)$ take values significantly smaller than the 19 others. This betrays linear dependencies amongst the 22 EEG-recordings. Indeed, time series result from subtraction amongst electrode measurements, some being used several times, so that one time series actually consists of the addition of several others. This leads to remove three redundant recordings from multivariate analysis, thus leading to a $M = 19$ multivariate self-similarity analysis, reported in Fig. 1(right).

Fig. 1 further confirms linear behaviors (hence scale-free dynamics) for both $\log_2 S_{m,m}(2^j)$ and log-eigenvalues $\log_2 \bar{\lambda}_m(2^j)$, $m = 1, \ldots, M$, at fine scales.

C. Self-similarity parameter estimate distributions

To illustrate the ability of self-similarity analysis to detect preictal states temporal dynamics from those of interictal states, Fig. 2 compares (by means of boxplots) the distributions of the univariate $\hat{H}_m^U$ (left) and eigen-wavelet multivariate $\hat{H}_m^M$ (right) estimates of the H_m, computed for the Subjects 5 (top) and 20 (bottom), from the 169 available interictal windows (blue) and the 15 available preictal windows (red). Fig. 2 shows clearer distinctions between the distributions of estimated preictal and interictal H_m, for each m, for the eigen-wavelet based $\hat{H}_m^M$, compared to univariate $\hat{H}_m^U$, with lower spreading in distribution and smaller overlap between distributions.

Fig. 2 also shows, by comparisons between subjects, that detection between interictal and preictal states must be performed on a per-subject basis. Indeed, the distributions of $\hat{H}_m$ for interictal states differ from one subject to the other, hence average across subjects would blur differences between preictal and interictal statistics. These observations are valid for all subjects (not shown here for space reasons). Fig. 2 clearly indicates that i) preictal states have temporal dynamics that departs from those of the interictal states of one same subject and ii) that interictal states of different subjects have different temporal dynamics. These are the first significant findings of this work.

To quantify differences amongst distributions of estimated self-similarity parameters between preictal and interictal states, Wilcoxon signed-rank test p-values p_m^W are computed. These p-values are compared to Benjamini-Hochberg (multiple hypothesis correction) thresholds, $d_\alpha^{(W,m)}$, at a false discovery rate set to $\alpha = 0.05$ [16]. To further quantify differences between the $\hat{H}_m^M$ and the $\hat{H}_m^U$, an across component overall performance score is defined as the normalized signed distance from the p-values p_m^W to the Benjamini-Hochberg thresholds $d_\alpha^{(W,m)}$, score $= \frac{1}{M}\sum_{m=1}^{M}(d_\alpha^{(W,m)} - p_m^W)$.

Fig. 3 compares, for each of the available 8 subjects, the p-values p_m^W for $\hat{H}_m^M$ (red) and $\hat{H}_m^U$ (blue), compared to the Benjamini-Hochberg thresholds $d_\alpha^{(W,m)}$ (black) and reports the corresponding scores. Fig. 3 shows that the eigen-wavelet multivariate $\hat{H}_m^M$ lead systematically to lower p-values and thus larger overall scores, and for some subjects significantly so. These findings confirm i) the statistically significant differences between the temporal dynamics of preictal and interictal states on a per-subject basis, and ii) the improved ability of

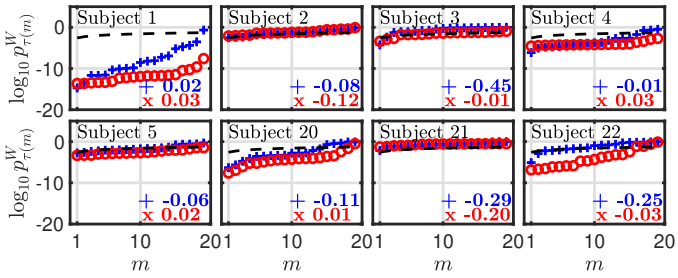

Fig. 3. **Comparisons of preictal and interictal estimated self-similarity parameters distributions.** Sorted log p-values of the Wilcoxon signed-rank test between preictal and interictal estimated self-similarity parameters distributions, and related scores, for univariate $\hat{H}^U_m$ (blue) and eigen-wavelet multivariate $\hat{H}^M_m$ (red) for the 8 different subjects, with the Benjamini-Hochberg (log-)thresholds (superimposed dashed black lines) at false discovery rate $\alpha = 0.05$.

the eigen-wavelet multivariate $\hat{H}^M_m$ to assess such differences.

D. Per subject preictal state detection performance

To further quantify the benefits of multivariate self-similarity analysis to detect preictal states on per-subject basis, ROC curves are computed as follows, for each subject independently. First, 100 interictal windows are selected randomly, from which self-similarity parameters are estimated and used to define the empirical distributions of the H_m under the null hypothesis (interictal state). Second, for all available N_w preictal windows and N_w interictal windows chosen randomly (not from the set of the 100 windows used to create the distributions under the null hypothesis), self-similarity parameters are estimated. Third, from these estimates, p-values are computed by comparisons against the distributions of estimates under null hypothesis and corresponding p-values are compared to Benjamini-Hochberg multiple comparison correction thresholds, for a collection of preset false discovery rates α. A (interictal state) rejection decision is taken as soon as one of the $M = 19$ p-values are lower than such threshold. Fourth, averaging these decisions across the N_w preictal and interictal windows permit to compute probabilities of correct detection and of false alarms for each preset false discovery rates α. These empirical probabilities are plotted one against the other to yield ROC curves.

This procedure is performed independently for the $M = 19$ univariate $\hat{H}^U_m$, for the $M = 19$ eigen-wavelet multivariate $\hat{H}^M_m$ and for the $M(M-1)/2 = 171$ classical multivariate $\hat{H}_{m,m'}$. Fig. 4 compares, for each of the 8 subjects independently, the resulting ROC curves and related area under curve (AUC) for the univariate $\hat{H}^U_m$ (blue lines with '+'), for the eigen-wavelet multivariate $\hat{H}^M_m$ (red lines with 'o') and for the classical multivariate $\hat{H}_{m,m'}$ (black lines with 'Δ'). Fig. 4 shows that the eigen-wavelet multivariate approach reaches overall the most satisfactory performance: First, it always outperforms the univariate strategy; Second, while it is outperformed by the classical multivariate strategy for one subject (Subject2), it essentially does as well as and sometimes significantly better (Subjects 21 and 22) than the classical multivariate strategy, which may show poor sensitivity, while performing only $M = 19$ instead of $M(M-1)/2 = 171$ tests.

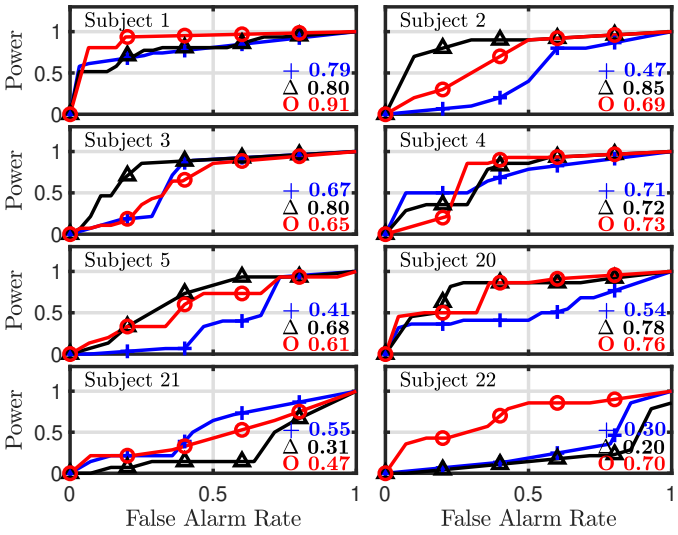

Fig. 4. **Epilepsy prediction from self-similarity exponent estimates.** ROC curves and related AUC of the test decisions for rejecting preictal states using (blue) univariate-like estimates $\hat{H}^U_m$, (black) classical multivariate estimates $\hat{H}^U_{m,m'}$ and (red) eigen-wavelet multivariate estimates $\hat{H}^M_m$ distributions for the different subjects.

V. Conclusion and Perspectives

The present work has shown the relevance of comparing, on a per-subject basis, the scale-free temporal dynamics of multichannel scalp EEG data, in intericatal and preictal states for epilectic seizure prediction. It has also shown that multivariate scale-free temporal dynamics assessed by a recently developed eigen-wavelet multivariate self-similarity analysis outperforms univariate or classical multivariate analyses.

Future work will include the design of a learning procedure for seizure prediction, using the multivariate self-similarity parameter estimates as features.

Matlab routines for multivariate self-similarity parameter estimation are publicly available at https://github.com/charlesglucas/ofbm_tools for sake of reproducibility.

References

[1] B. J. He, "Scale-free properties of the functional magnetic resonance imaging signal during rest and task," *J. Neurosci.*, vol. 31, no. 39, pp. 13786–13795, 2011.

[2] D. La Rocca, N. Zilber, P. Abry, V. van Wassenhove, and P. Ciuciu, "Self-similarity and multifractality in human brain activity: A wavelet-based analysis of scale-free brain dynamics," *J. Neurosci. Methods*, vol. 309, pp. 175–187, 2018.

[3] V. Pipiras and M. S. Taqqu, *Long-Range Dependence and Self-Similarity*, vol. 45, Cambridge University Press, 2017.

[4] P. Abry and G. Didier, "Wavelet estimation for operator fractional Brownian motion," *Bernoulli*, vol. 24, no. 2, pp. 895–928, 2018.

[5] G. MohanBabu, S. Anupallavi, and S. R. Ashokkumar, "An optimized deep learning network model for eeg based seizure classification using synchronization and functional connectivity measures," *Journal of Ambient Intelligence and Humanized Computing*, vol. 12, no. 7, pp. 7139–7151, 2021.

[6] F. Mormann, K. Lehnertz, P. David, and C.E. Elger, "Mean phase coherence as a measure for phase synchronization and its application to the eeg of epilepsy patients," *Physica D: Nonlinear Phenomena*, vol. 144, no. 3-4, pp. 358–369, 2000.

[7] K. K. Zhang, Z.and Parhi, "Low-complexity seizure prediction from ieeg/seeg using spectral power and ratios of spectral power," *IEEE transactions on biomedical circuits and systems*, vol. 10, no. 3, pp. 693–706, 2015.

[8] M. E. Saab and J. Gotman, "A system to detect the onset of epileptic seizures in scalp eeg," *Clinical Neurophysiology*, vol. 116, no. 2, pp. 427–442, 2005.

[9] L. Chisci, A. Mavino, G. Perferi, M. Sciandrone, C. Anile, G. Colicchio, and F. Fuggetta, "Real-time epileptic seizure prediction using ar models and support vector machines," *IEEE Transactions on Biomedical Engineering*, vol. 57, no. 5, pp. 1124–1132, 2010.

[10] H. Daoud and M. A. Bayoumi, "Efficient epileptic seizure prediction based on deep learning," *IEEE transactions on biomedical circuits and systems*, vol. 13, no. 5, pp. 804–813, 2019.

[11] K. Gadhoumi, J. Gotman, and J.-M. Lina, "Scale invariance properties of intracerebral eeg improve seizure prediction in mesial temporal lobe epilepsy," *PLoS one*, vol. 10, no. 4, pp. e0121182, 2015.

[12] O. D. Domingues, P. Ciuciu, D. La Rocca, P. Abry, and H. Wendt, "Multifractal analysis for cumulant-based epileptic seizure detection in eeg time series," in *2019 IEEE 16th International Symposium on Biomedical Imaging (ISBI 2019)*. IEEE, 2019, pp. 143–146.

[13] C.-G. Lucas, P. Abry, H. Wendt, and G. Didier, "Bootstrap for testing the equality of selfsimilarity exponents across multivariate time series," in *Proc. European Signal Processing Conference (EUSIPCO)*, Dublin, IE, August 2021.

[14] A. L. Goldberger, L. A. Amaral, L. Glass, J. M. Hausdorff, P. C. Ivanov, R. G. Mark, J. E. Mietus, G. B. Moody, C. K. Peng, and H. E. Stanley, "Physiobank, physiotoolkit, and physionet: components of a new research resource for complex physiologic signals," *circulation*, vol. 101, no. 23, pp. e215–e220, 2000.

[15] S. Mallat, *A Wavelet Tour of Signal Processing*, Academic Press, San Diego, CA, 1998.

[16] Y. Benjamini and Y. Hochberg, "Controlling the false discovery rate: a practical and powerful approach to multiple testing," *Journal of the Royal statistical society: series B (Methodological)*, vol. 57, no. 1, pp. 289–300, 1995.